

# The formation of stable hydrogen impermeable TiN-based coatings on zirconium alloy Zr1%Nb

E B Kashkarov<sup>1</sup>, N N Nikitenkov<sup>1</sup>, Yu I Tyurin<sup>1</sup>, M S Syrtanov<sup>1</sup>, Zhang Le<sup>1</sup>

<sup>1</sup>Tomsk Polytechnic University, 30 Lenin Avenue, Tomsk, Russian Federation

E-mail: egor\_kashkarov@mail.ru

**Abstract.** TiN coatings were deposited by DC reactive magnetron sputtering (dcMS) method on Zr1%Nb substrates with different film thickness. The influence of crystalline structure and thickness of the coatings on hydrogen permeation was investigated. The results revealed that the increase in thickness of the film reduced hydrogen permeability. 1.54  $\mu\text{m}$  TiN deposited in  $\text{N}_2/\text{Ar}$  gas mixture with a ratio of 3/1 reduces hydrogen permeation in more than two orders of magnitude at 350 °C. Adhesion strength decreased with increasing film thickness (0.55 to 2.04  $\mu\text{m}$ ) from 7.92 to 6.65 N, respectively. The Ti underlayer applied by arc ion plating (AIP) leads to the formation of stable Ti/TiN coatings on Zr1%Nb under thermocycling conditions up to 800 °C. Meanwhile, hydrogen permeation rate of Ti/TiN deposited by combination of AIP and dcMS remains at the same level with TiN deposited by dcMS.

## 1. Introduction

The problem of protection of structural and functional materials operating in hydrogen-containing ambient in nuclear reactors and fuel cells is very important. In Russian Water-Water Energetic Reactor (WWER) and High Power Channel Reactor (RBMK) the Zr1%Nb alloy is used as a cladding material. Zirconium and its alloys are susceptible to hydrogen corrosion and fretting wear. It is known that the certain concentrations of hydrogen in the bulk of the material leads to embrittlement and subsequent degradation of mechanical properties [1–6]. Titanium nitride (TiN) deposited by vacuum ion-plasma methods is promising in protection zirconium alloys from hydrogen corrosion [7]. Moreover, TiN coatings have an excellent erosion resistance, which favorably affects the fretting resistance of the coatings [8]. There is no scientific data in information about hydrogen sorption kinetics by TiN coated zirconium alloy by dcMS method. At the same time, such studies are of great practical importance for the development of TiN coating technology, allowing to work in extremal conditions.

One of the most important tasks in the development of coating technology is to ensure good adhesion of the coating under thermal cycling. The differences between temperature expansion coefficient of the coating and substrate materials leads to the coating degradation and various accidents can occur. In this paper the problem of stability of the coatings under thermal cycling was solved by creating a Ti underlayer deposited by AIP between the zirconium alloy Zr1%Nb and magnetron sputtered TiN.

The aim of this work is to create a stable hydrogen-impermeable TiN-based protective coating under thermocycling conditions using the AIP and dcMS methods.

## 2. Experimental Procedure



The Zr1%Nb alloy is used as the substrate that fixed size is 0.5 mm thickness and 20 mm diameter. The samples were previously polished using sandpaper to a roughness 0.1  $\mu\text{m}$ . The Ti underlayer and TiN coatings were deposited in a hybrid «Arc spectrum» technique which was developed in Tomsk Polytechnic University. Vacuum arc evaporator with coaxial plasma filter (designed by authors [9,10]) was used for AIP method. Firstly, the chamber was evacuated to a base pressure of lower, than  $2.5 \times 10^{-3}$  Pa. Before deposition, samples were subjected to ion bombardment in an argon glow discharge at 1500 V for 5 min.

Process parameters for AIP of Ti underlayer: arc current – 110 A; pulsed substrate bias – (-150 V); pulse repetition frequency – 100 kHz; peak pulse current – 3 A; Ar pressure –  $2 \times 10^{-1}$  Pa.

The TiN coatings were reactively sputtered in mixed  $\text{N}_2/\text{Ar}$  gases with different ratio (1/1, 2/3, 1/3, 1/4). Pressure in the chamber remained constant  $1.54 \times 10^{-1}$  Pa. Sputtering power and current was 2.6 kW and 4 A, respectively. The deposition time was varied from 10 min to 40 min.

Hydrogenation of the samples was performed by Sievert method (from hydrogen atmosphere) during 60 min at temperature 350  $^{\circ}\text{C}$  (heating rate 6  $^{\circ}\text{C}/\text{min}$ ) and 2 atm hydrogen pressure. The hydrogenation temperature was chosen due to working temperature of zirconium fuel cladding in the operation process of nuclear reactors.

Hydrogen sorption kinetics was measured by Sievert method with automated complex Gas Reaction Controller. The phase constitutions of the deposited films were identified by X-ray diffraction (Shimadzu XRD-7000) using  $\text{Cu K}\alpha$  radiation (1.5410 Å wavelength) generated at 40 kV and 30 mA with the fixed angle ( $\theta=3^{\circ}$ ). The film thickness was measured by simple ball-cratering method performed with Calotest CAT-S-0000. The adhesion strength was measured by scratch method using Micro Scratch Tester MST-S-0000.

### 3. Results and Discussion

#### 3.1. Crystalline structure and hydrogen permeation of TiN coatings deposited at the different $\text{N}_2/\text{Ar}$ ratio

Titanium nitride thin films were deposited by reactive dcMS method in mixed  $\text{N}_2/\text{Ar}$  gases with different ratio. The process parameters are shown in Table 1.

**Table 1.** Process parameters for TiN coatings deposition

Sample	Pressure P, $10^{-1}$ Pa	DC current I, A	Power W, kW	Deposition time t, min	$\text{N}_2/\text{Ar}$ ratio
1	1.54	4	2.6	30	1/1
2	1.54	4	2.6	30	3/2
3	1.54	4	2.6	30	3/1
4	1.54	4	2.6	30	4/1

Figure 1 shows the XRD patterns of TiN coatings applied on Zr1%Nb substrates as a function of the  $\text{N}_2/\text{Ar}$  ratio. It is seen that the difference of the TiN coatings with increasing  $\text{N}_2/\text{Ar}$  ratio is not significant. In all cases, the crystalline structure of the TiN coatings is cubical (type NaCl) and it is possible to see that the orientation in the plane (200) is the reflection of major intensity and it remains as the most intense from 1/1 to 4/1  $\text{N}_2/\text{Ar}$  ratio. Similar results in preferred TiN orientation in plane (200) have also been observed in report [11]. The less intensive (220) and (222) reflections have been observed. The reflections in plane (111) are difficult to resolve due to the merger with substrate (Zr) reflections. Plane (111) and plane (200) have the lowest strain energy and the lowest surface energy in NaCl-type fcc nitrides, respectively. The fact that the preferential direction is (200) can be explained from investigations that Pelleg et al. made [12], which were later confirmed by Oh et al. [13,14].

The more intensive (200) reflection have been observed for the sample which was deposited at 3/1  $\text{N}_2/\text{Ar}$  ratio compared to other samples. Furthermore, the intensity of TiN in the plane (111) and zirconium reflections decreased. It could be connected with the fact that the crystalline lattice of this

sample is more preferentially oriented in the plane (200) or associated with zirconium substrate texture.

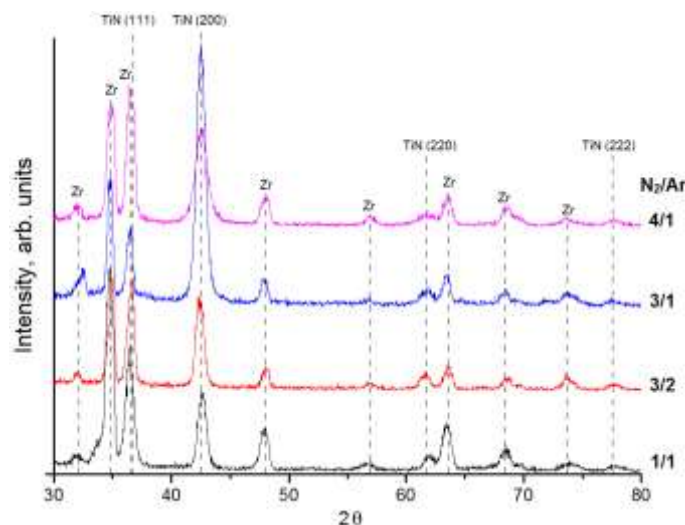


**Figure 1.** XRD analysis of TiN coatings deposited at different N<sub>2</sub>/Ar ratio

Hydrogenation of the samples was performed at temperature 350 °C and hydrogen pressure 2 atm during 60 min. The TiN coatings deposited with 1/1 and 3/2 N<sub>2</sub>/Ar ratio were destroyed as a result of hydrogen embrittlement of zirconium alloy. There are no discontinuities for the TiN coatings deposited with 3/1 and 4/1 N<sub>2</sub>/Ar ratio have been observed under optical microscope.

The decrease in the hydrogen pressure in the chamber indicates the hydrogen absorption process by the samples. The slope of the «pressure-time» curve measured in the saturation process of the samples characterizes the intensity of the hydrogen absorption. The hydrogen absorption rate is calculated by the following formula:

$$q = \frac{V}{t \cdot S} \ln(P/P_0) \quad (1)$$

where  $V$  – chamber volume (175 cm<sup>3</sup>),  $t$  – saturation time,  $S$  – effective surface area of the sample,  $P$  и  $P_0$  – final and initial hydrogen pressure in the chamber, respectively.

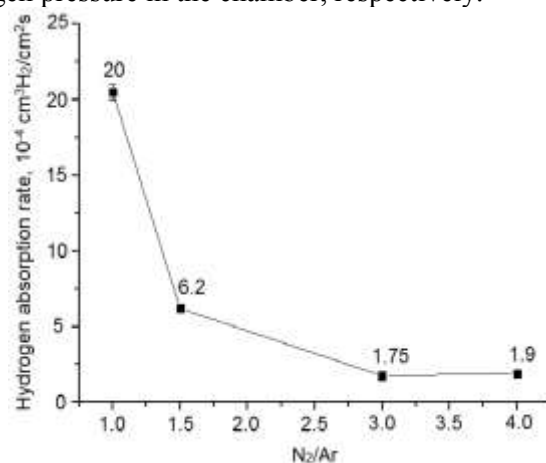


**Figure 2.** Hydrogen absorption rate by TiN deposited at different N<sub>2</sub>/Ar ratio (numbers near the points correspond to exact values)

The hydrogen absorption rate which characterizes hydrogen permeation was calculated by the formula (1). Figure 2 shows that the hydrogen absorption rate decreased with increasing N<sub>2</sub>/Ar ratio

up to 3/1 and then insignificantly increase in the hydrogen absorption rate was observed. Therefore, TiN coatings deposited on our hybrid technique by reactive dcMS method with 3/1 N<sub>2</sub>/Ar ratio have the lowest hydrogen permeability. It appears that the highest hydrogen absorption rate for the samples with TiN deposited at gas mixture N<sub>2</sub>/Ar < 3/1 has a high structural defects formed during deposition.

### 3.2. The influence of TiN thickness on hydrogen permeability and adhesion strength of the coatings

To study the effect of TiN coating thickness on the hydrogen permeability hydrogen absorption rate have also been measured. Deposition time was varied from 10 to 40 min to change the film thickness. The N<sub>2</sub>/Ar=3/1 ratio was defined in terms of lowest hydrogen permeability of TiN. The thickness of the deposited coatings was measured by simple ball-cratering method using Calotest CAT-S technique. Figure 3 shows the linear dependence between the thickness of TiN coatings and deposition time. Deposition rate is 3  $\mu\text{m}$  in this magnetron sputtering parameters.

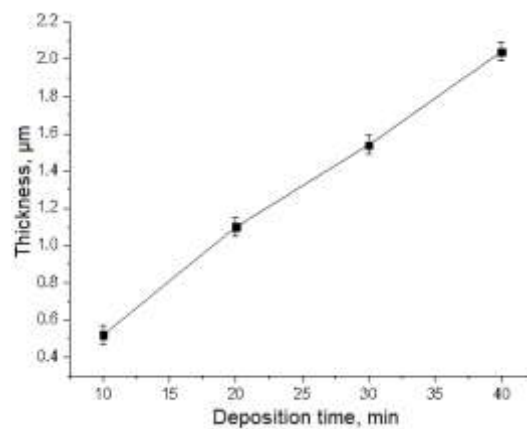


**Figure 3.** Thickness of the TiN

The hydrogen absorption rate was calculated for the samples with different TiN thickness and is shown in Figure 4. It can be seen that increasing the coating thickness leads to a reduction of the hydrogen absorption rate.

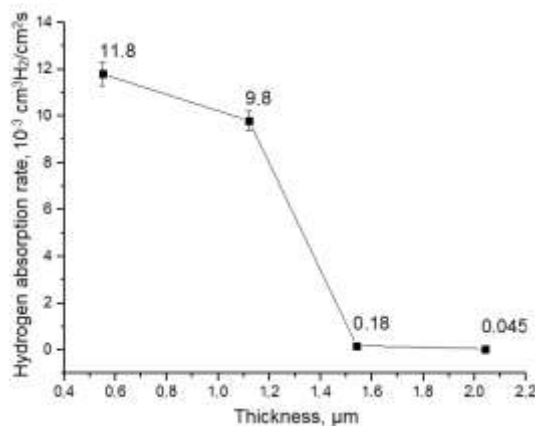


**Figure 4.** Hydrogen absorption rate by TiN deposited with different thickness (numbers near the points correspond to exact values)

The hydrogen absorption rate is  $12 \times 10^{-3} \text{ cm}^3 \text{ H}_2 / (\text{cm}^2 \cdot \text{s})$  for the Zr1%Nb alloy without coatings. Thus, the hydrogen differently interacts with the TiN coatings of various thickness. It can be seen that the hydrogen absorption rate insignificantly reduced for the 0.5–1  $\mu\text{m}$  TiN coatings compared to uncoated zirconium alloy. The reduction of hydrogen absorption rate in 50–60 times and more than two orders of magnitude was observed for 1.54  $\mu\text{m}$  and 2.04  $\mu\text{m}$  TiN, respectively. The hydrogen absorption rate for the TiN coatings has also been evaluated in reports [15], where the reduction of

more than 2 orders of magnitude was observed only for 7–9  $\mu\text{m}$  TiN coatings and the hydrogen absorption rate was negligible for 1–2  $\mu\text{m}$  TiN.

The measurement of adhesion strength was performed with MicroScratchTester MST-S-AX-0000 technique by scratch method using a diamond indenter. Scratching parameters: initial load – 0.01 N; ultimate load – 20 N; scratching speed – 9.63 mm/min; scratch length – 10 mm. The measuring results are shown in Table 2.

**Table 2.** Adhesion strength of TiN

Thickness, $\mu\text{m}$	0.55	1.12	1.54	2.04
Adhesion strength, N	7.92	7.67	7.51	6.65

Table 2 shows that the adhesion strength of the TiN coatings deposited by dcMS method decreases with increasing coating thickness. The adhesion strength decreased from 7.92 to 6.65 N for the 0.55 to 1.54  $\mu\text{m}$  TiN thickness, respectively.

Low adhesion strength of TiN coatings (<6 N for scratch method) along with the difference in temperature expansion coefficients of titanium nitride and zirconium alloy leads to coating delamination (detachment) during thermal cycling. Thus, a further increase in TiN thickness is impractical from the viewpoint of thermal stability and adhesion strength of the coatings.

### 3.3. The formation of stable Ti/TiN deposited by AIP and dcMS methods

In this paper the problem of low adhesion strength of TiN coatings and the difference between temperature expansion coefficients for TiN and Zr1%Nb was solved by applying a Ti underlayer using AIP technique.

The basis for this approach includes the following general considerations. It is known [17] that AIP of one metal to another metal may lead to the formation of the various intermetallic phases. In this report the phase composition of the surface after AIP has not been investigated. However, the formation of different Ti-Zr phases at AIP is possible, for example [18]. It seems that it will promote the balancing temperature expansion coefficient between the substrate and the coating and improve the adhesion strength.

The Ti underlayer was deposited using AIP at 110 A arc current and -150 V pulsed (100 kHz) substrate bias. Then, the 1.54  $\mu\text{m}$  TiN coating was deposited by dcMS method with  $\text{N}_2/\text{Ar}=3/1$  ratio at the same parameters shown in Table 1.

The adhesion strength and the hydrogen permeability of Ti/TiN were investigated before and after thermocycling.

Thermocycling of the samples was performed with a water cooled vacuum furnace. The residual pressure in the chamber was  $(6-7) \times 10^{-3}$  Pa. Heating and cooling rates were 200 and  $\sim 2000$   $^{\circ}\text{C}/\text{min}$ , respectively. Three cycles of heating and cooling the Zr1%Nb samples coated with TiN and Ti/TiN were performed. After cooling, the samples were removed from the vacuum furnace.

The surface of the sample without underlayer contained peeling of the coating and cracks formed during thermal expansion, which was not observed in the sample with a Ti underlayer.

Hydrogen saturation of the samples with Ti/TiN coatings was performed after thermocycling at following conditions:  $T = 350$   $^{\circ}\text{C}$ ,  $P = 2$  atm,  $t = 60$  min. The hydrogen absorption rate of Zr1%Nb alloy coated with TiN (before thermal cycling) and Ti/TiN (after thermal cycling) was calculated. The results are shown in the Table 3.

**Table 3.** Hydrogen absorption rate of TiN and Ti/TiN coatings

Sample	Zr1%Nb+TiN	Zr1%Nb+Ti/TiN
Hydrogen absorption rate, $\times 10^{-4} \text{ cm}^3 \text{ H}_2/(\text{cm}^2\text{s})$	1.75	1.64

After thermocycling the hydrogen absorption rate of Ti/TiN is lower than TiN without underlayer. This is evidence of an minimal reduction in the hydrogen permeability induced by additional Ti underlayer diffusion barrier or changes in the structure of the TiN coating.

Before and after thermocycling three measurements of the adhesion strength were performed for each samples using the same method as described above. The adhesion strength of the TiN deposited by dcMS after thermal cycling is reduced from 7.75 N to 4.46 N; at the same time for the samples with Ti underlayer the adhesion strength is remained at the same level before and after thermal cycling. This result demonstrates that the TiN coating with Ti underlayer is resistant when exposed to rapidly changing temperatures in the range of 20–800 °C.

#### 4. Conclusion

The study has demonstrated that the vacuum ion-plasma TiN coatings deposited by reactive magnetron sputtering lead to the reduction of hydrogen permeation through zirconium alloys. The decrease in the hydrogen absorption rate in more than two order of magnitude was observed for 2 µm TiN coating deposited at N<sub>2</sub>/Ar = 3/1 ratio. The magnetron sputtered TiN has a cubic lattice with the (200) preferred orientation.

The adhesion strength of TiN was improved by applying a Ti underlayer using arc ion plating technique. The combination of AIP and reactive dcMS methods leads to the formation of Ti/TiN coatings which are resistant during thermal cycling in the temperature range of 20–800 °C. The hydrogen permeation rate of Ti/TiN remains at the same level with TiN deposited by dcMS. The investigated coatings are perspective to protect zirconium alloys from the hydrogen embrittlement.

#### References

- [1] Chernyaeva T P, Ostapov A V 2013 *Voprosy atomnoy nauki i tehniki* **87** 16
- [2] Silva K R F, DosSantos D S, Robeiro A F, Almeida L H 2010 *Defect and Diffusion Forum* **297–301** 722
- [3] Zielinski A, Sobieszczyk S 2011 *Intern. Journ. of Hydrogen Energy* **36** 8619
- [4] Bai J B 1993 *Scripta Metallurgica et Materialia* **29** 1259
- [5] Mani Krishna K V, Sain A, Samajdar I, Dey G K et al. 2006 *Acta Materialia* **54** 4665
- [6] Singh R N, Kishore R, Singh S S, Sinha T K, Kashyap B P 2004 *Journ. of Nuclear Materials* **325** 26
- [7] Ivanova S V, Glagovskiy E M, Khazov I A, Orlov V K, Shlepov I A, Nikitin K N, Dubrovskiy Yu V, Denisov E A 2008 *Proc. IV Int. Conf. on Interaction of Hydrogen Isotopes with Structural Materials (Nizhny Novgorod)* p 51
- [8] Aleksandrov D A, Gorlov D S, Zhuravleva P L, Lutsenko A N, Muboyadzhyan S A 2011 *Metally* **4** 91
- [9] Ryabchikov A I, Ryabchikov I A, Stepanov I B 2005 *Vacuum* **78** 331
- [10] Ryabchikov A I and Stepanov I B 2009 *Surface and Coating Technology* **203** 2784
- [11] Chun S Y 2010 *Journal of the Korean Physical Society* **56** 1134
- [12] Pelleg J, Zevin L Z, Lungo S, Croitoru N 1991 *Thin Solid Films* **197** 117
- [13] Oh U C, Je J H 1993 *J. Appl. Phys.* **74** 1692
- [14] Oh U C, Je J H, Lee J Y 1995 *J. Mater. Res.* **10** 634
- [15] Selezneva L V, Bushmin B V, Dubrovskiy Yu V, Khazov I A, Denisov E A, Kurdyumov A A 2008 *Voprosy atomnoy nauki i tehniki* **2** 108
- [16] Kurzina I A, Bozhko I A, Kalashnikov M P, Fortuna S V, Batyreva V A, Stepanov I B, Sharkeev Yu P 2004 *Bulletin of Tomsk Polytechnic University* **307** 30
- [17] Bovda A M, Dmitrenko A E, Malyhin D G, Onishchenko L V, Pelyh V N 2007 *Voprosy atomnoy nauki i tehniki* **4** 173